Effects of Glucosamine Infusion on Insulin Secretion and Insulin Action in Humans

Tiziano Monauni, Maria Grazia Zenti, Anna Cretti, Marc C. Daniels, Giovanni Targher, Beatrice Caruso, Marco Caputo, Donald McClain, Stefano Del Prato, Andrea Giaccari, Michele Muggeo, Enzo Bonora, and Riccardo C. Bonadonna

Glucose toxicity (i.e., glucose-induced reduction in insulin secretion and action) may be mediated by an increased flux through the hexosamine-phosphate pathway. Glucosamine (GlcN) is widely used to accelerate the hexosamine pathway flux, independently of glucose. We tested the hypothesis that GlcN can affect insulin secretion and/or action in humans. In 10 healthy subjects, we sequentially performed an intravenous glucose (plus [2-^{3}H]glucose) tolerance test (IVGTT) and a euglycemic insulin clamp during either a saline infusion or a low (1.6 µmol · min^{-1} · kg^{-1}) or high (5 µmol · min^{-1} · kg^{-1} [n = 5]) GlcN infusion. β-Cell secretion, insulin (S_I*-IVGTT), and glucose (S_G*) action on glucose utilization during the IVGTT were measured according to minimal models of insulin secretion and action. Infusion of GlcN did not affect readily releasable insulin levels, glucose-stimulated insulin secretion (GSIS), or the time constant of secretion, but it increased both the glucose threshold of GSIS (Δ ~0.5–0.8 mmol/l, P < 0.03–0.01) and plasma fasting glucose levels (Δ ~0.3–0.5 mmol/l, P < 0.05–0.02). GlcN did not change glucose utilization or intracellular metabolism (glucose oxidation and glucose storage were measured by indirect calorimetry) during the clamp. However, high levels of GlcN caused a decrease in S_I*-IVGTT (Δ ~30%, P < 0.02) and in S_G* (Δ ~40%, P < 0.05). Thus, in humans, acute GlcN infusion recapitulates some metabolic features of human diabetes. It remains to be determined whether acceleration of the hexosamine pathway can cause insulin resistance at euglycemia in humans. *Diabetes* 49:926–935, 2000

From the Division of Endocrinology and Metabolic Diseases (T.M., M.G.Z., A.C., G.T., M.M., E.B., R.C.B.), University of Verona School of Medicine and the Clinical Chemistry and Hematology Laboratories (B.C., M.C.), Verona City Hospital, Verona; the Division of Metabolic Diseases (S.D.P.), University of Padua School of Medicine, Padua; the Division of Endocrinology (A.G.), Catholic University School of Medicine, Rome, Italy; the Department of Molecular Physiology and Biophysics (M.C.D.), Vanderbilt University Medical Center, Nashville, Tennessee; and the Division of Endocrinology (D.M.), Veterans Administration and University of Utah School of Medicine, Salt Lake City, Utah.

Address correspondence and reprint requests to Riccardo C. Bonadonna, MD, Division of Endocrinology, Ospedale Civile Maggiore, Piazzale Stefani 1, I37126 Verona, Italy. E-mail: rcbonado@tin.it.

Received for publication 22 November 1999 and accepted in revised form 17 February 2000.

ANOVA, analysis of variance; CV, coefficient of variation; EGO, endogenous glucose output; FFA, free fatty acid; GFAT, glutamine fructose-6-phosphate amidotransferase; GlcN, glucosamine; GSIS, glucose-stimulated insulin secretion; HPLC, high-performance liquid chromatography; IVGTT, intravenous glucose tolerance test; RRI, readily releasable insulin; S_G*, glucose effectiveness obtained with a glucose tracer; S_I, insulin sensitivity, S_I*-IVGTT, insulin action.

As first suggested by Unger and Grundy several years ago (1), hyperglycemia exerts detrimental effects on insulin secretion and insulin action, a phenomenon commonly referred to as glucose toxicity (2). Subsequent elegant studies conducted in rat adipocytes in vitro led several authors to propose that insulin resistance induced by cell exposure to high levels of glucose was due to the acceleration of the hexosamine pathway, a quantitatively minor route of fructose-6-phosphate and, hence, glucose disposal (3–5).

Glutamine fructose-6-phosphate amidotransferase (GFAT) is the key enzyme that regulates the flux through the hexosamine pathway, which marks the first step in hexosamine biosynthesis, as glutamine and fructose-6-phosphate is converted to glucosamine-6-phosphate. GFAT is widely expressed in human tissues such as muscle, fat, vascular smooth muscle cells, liver, and pancreatic islet cells (6). The nature of the signal downstream to GFAT, which affects insulin action, is somewhat elusive, but the signal leads to an impairment in insulin-induced GLUT4 translocation (7,8) and glycogen synthase activation (9–11), which is possibly secondary to an inhibition of the early steps in insulin signaling (12–14) and to a stimulation of protein kinase C (15).

Acceleration in vivo of the hexosamine pathway, which is achieved by glucosamine (GlcN) (7,13,14,16–20), uridine (21), high free fatty acid (FFA) (21) and glucose levels (16), and GLUT1 (22) or GFAT overexpression (23), leads to insulin resistance in the rat through inhibition of the transport/phosphorylation step (16,17) and a specific impairment in insulin-mediated intracellular trafficking of GLUT4 in skeletal muscle (7,8). Therefore, several investigators (4,21,24,25) have proposed that the hexosamine pathway acts as a fuel sensor in insulin-sensitive cells, so that when the cell is inundated with substrates (i.e., glucose and/or FFAs), insulin resistance develops and prevents cell engorgement by oxidizable compounds. Acceleration of the hexosamine pathway also causes leptin expression in skeletal muscle (25), which, by regulating appetite and route of fat disposal, could potentially close a negative feedback loop and inhibit the self-maintenance of a vicious cycle between lipid/glucose excess and insulin resistance (26). Alterations in this feedback system eventually lead to a break in glucose homeostasis (24). Accordingly, increased GFAT activity has been found in both animal (27,28) and human diabetes (29,30).

GlcN has been the most widely used tool to increase the flux through the hexosamine-phosphate pathway (7,13,14,16–20), because it is metabolized to glucosamine-6-phosphate by the couple glucose transporter/hexokinase, thereby bypassing GFAT and leading to a glucose-independent increase in the pathway flux.

However, some studies have reported data not perfectly fitting with the GlcN/GFAT paradigm. For instance, GlcN may also impair the early steps of insulin signaling by depleting ATP, a mechanism not known to be shared by glucose (12). However, both GlcN and GFAT overexpression cause insulin resistance in vivo with no depletion of tissue ATP (8,14). GlcN impairs insulin stimulation of phosphatidylinositol 3-kinase, but not Akt/protein kinase B (13,14), a subsequent signaling step considered to be important for insulin-mediated GLUT4 translocation (31). Troglitazone prevents glucose- but not GlcN-induced insulin resistance, suggesting that different mechanisms underlie insulin resistance in these 2 models (32). On the other hand, troglitazone can impede the appearance of insulin resistance in mice overexpressing GFAT, which is in agreement with the hexosamine hypothesis (8). After exercise, at a time when insulin sensitivity is increased, a paradoxical increase in the muscle levels of the products of the hexosamine-biosynthetic pathway is observed (33). Some of these inconsistencies may, at least partially, be explained by the finding that in skeletal muscle, GlcN infusion, but not diabetes, leads to a marked accumulation of GlcN-6-phosphate, which in turn exerts opposite effects of its own on glycogen synthase and hexokinase (34).

A further, though less studied, aspect of the GlcN paradigm is relevant to β-cell secretion. GlcN has long been known to be an inhibitor of glucokinase (35–37), the glucose sensor of the β-cell. Accordingly, GlcN in vivo can reduce the first and second phases of insulin secretion in the rat (17,37,38), suggesting that it can fully mimic the detrimental effect of prolonged glucose exposure on insulin action and secretion (17,38).

Furthermore, GlcN is being marketed to treat osteoarthritis, and it might have harmful effects on glucose homeostasis in these patients, who frequently are elderly and/or obese (39).

Thus, considering the great importance that the GlcN/hexosamine paradigm may have in human disease, we undertook the present investigation to ascertain whether GlcN administration can affect insulin secretion and insulin action in normal healthy people.

RESEARCH DESIGN AND METHODS

Subjects. Ten healthy young male volunteers (aged 24.9 ± 0.43 years, BMI 23.5 ± 0.81 kg/m^2) were studied. The subjects consumed a weight-maintaining diet that contained 200–250 g carbohydrate per day for at least 3 days before the study. Body weight was stable in all of the subjects for at least 3 months before the study. No subject was taking any medication, and there was no family history of diabetes. No subject participated in any heavy exercise. All subjects had a normal oral glucose tolerance test (40). Each subject gave informed written consent before participating in the study, which was approved by the Human Investigation Committee of the Verona City Hospital.

Experimental design. At 8:30 A.M., after a 10–12 h overnight fast, subjects were admitted to the Clinical Research Center. Each subject participated in 2 or 3 studies, which were performed in random order and were 1–3 weeks apart. Catheters were introduced into an antecubital vein for the infusion of test substances, and they were introduced retrogradely into a wrist vein to sample arterialized venous blood. The hand was placed in a heated box (60°C) during the study to ensure arterialization of the venous blood. Catheter patency was maintained by filling the catheters with mildly heparinized saline solution. Each study lasted 360 min (–60 to 300). At –60 min, a primed continuous infusion of normal saline (saline study, ***n*** = 10) or GlcN (low GlcN study 1.6 μmol · min^{-1} · kg^{-1} body wt, ***n*** = 10) was started and continued until the end of the study. Five subjects agreed to participate in a third study (the high GlcN study), in which GlcN was administered at the rate of 5 μmol · min^{-1} · kg^{-1}. At these GlcN doses, no untoward effects were noticed in the study participants, with the exception of 1 subject who complained of having a headache during the last hour of study. At 0 min, an intravenous glucose tolerance test (IVGTT) (1.67 mmol glucose/kg body wt plus high-performance liquid chromatography [HPLC]-purified [2-^{3}H]glucose aiming at a glucose specific activity of ~2 μCi/g) was performed. The glucose load (50% dextrose solution) was administered over 35–45 s with a volumetric Harvard pump (Harvard Apparatus, South Natick, MA), and it was followed by 50 ml normal saline to flush the catheter and the antecubital vein. Blood samples were collected at baseline and at 1, 2, 3, 4, 5, 6, 8, 10, 12, 15, 20, 25, 30, 35, 40, 60, 80, 100, 120, 140, 160, 170, and 180 min to measure plasma glucose, [2-^{3}H]glucose, serum insulin, and C-peptide concentrations. In 1 subject who participated in only 2 studies, [2-^{3}H]glucose was not added to the intravenous glucose load because of a technical error.

At 180 min, when both glucose and insulin concentrations had returned to baseline values, a euglycemic insulin clamp was carried out for 120 min (41). It has been shown that sequentially performing an IVGTT and a euglycemic insulin clamp has no effects on the results of the clamp (42). Human insulin (Actrapid; Novo Nordisk, Rome, Italy) was infused at the constant rate of 6 pmol · min^{-1} · kg^{-1} body wt, preceded by an intravenous prime at 180 min of 120 pmol/kg body wt. The plasma glucose concentration was maintained constant at the target level by determining the plasma glucose concentration every 5 min and by adjusting the infusion rate of a 20% glucose solution according to a negative feedback principle. The glucose infusion was started in each of the studies at 180 min at the initial rate of 5.5 μmol · min^{-1} · kg^{-1} body wt. The target glucose concentration of the clamp was the clamp glucose concentration of the study that was performed first. To estimate endogenous glucose production, 100 μCi of HPLC-purified [2-^{3}H]glucose was added to the 20% dextrose solution (500 ml) used to perform the clamp, so that the expected glucose specific activity of the dextrose solution was ~1 μCi/g. To hasten the attainment of isotopic steady state, at 180 min a [2-^{3}H]glucose bolus was administered intravenously. The size of the [2-^{3}H]glucose bolus was calculated according to the following formula, which was empirically derived during pilot studies:

$$\text{Bolus of [2-}^3\text{H]glucose (μCi)} = 3 \times \text{glucose pool (g)} \times 1\ \text{μCi/g}$$

where the glucose pool was assumed to equal the product of plasma glucose concentration (g/l) times 0.25 of body weight (kg), and 1 μCi/g was the approximate specific activity of the 20% dextrose solution (43).

During the insulin clamp, blood was drawn at 190, 200, 210, 220, 240, 260, 280, 290, and 300 min to measure plasma glucose specific activity and insulin, lactate, and FFA levels. Throughout the study, blood was drawn at time intervals to determine the prevailing concentrations of GlcN. All blood samples were collected in prechilled tubes, promptly spun at 1,500***g*** for 15 min at 4°C, decanted, and stored at –20°C.

Both at baseline (–60 to 0 min) and during the last hour of the clamp (240–300 min), substrate oxidation rates were estimated by computerized open-circuit indirect calorimetry (Deltatrac; Datex, Helsinki, Finland). Timed (–60 to 0, 0 to 180, and 180 to 300 min) urine collections were performed to measure the excretion rates of urea, GlcN, and glucose.

Materials. Cell culture–tested D(+)-GlcN was purchased from Sigma-Aldrich (Milan, Italy). Stock solutions of highly concentrated GlcN were prepared by dissolving GlcN in normal saline and, after being filtered through a sterile 0.22-μm filter, were tested to be sterile and pyrogen-free and then stored at –20°C for no longer than 4 weeks before use. On the morning of each study, 1 stock solution was thawed and diluted into a 250-ml bottle of normal saline under sterile conditions. HPLC-purified [2-^{3}H]glucose was purchased from NEN Life Science Products (Boston, MA) and was tested to be sterile and pyrogen-free before use.

Analytical methods. Serum insulin and C-peptide concentrations were measured by an immunoradiometric assay (Insulin-IRMA; Medgenix Diagnostics, Fleurus, Belgium) and a radioimmunoassay (C-peptide Myria; Techno-Genetics, Milan, Italy), respectively. Plasma glucose concentrations were measured in duplicate on a Beckman Glucose Analyzer II (Beckman Instruments, Fullerton, CA). Plasma samples for the determination of [2-^{3}H]-D-glucose concentrations were deproteinized according to the method described by Somogyi (43a) and were dried, reconstituted with water, and mixed with scintillation fluid (Ultima Gold; Packard Instruments, Downers Grove, IL). Radioactivity was quantitated in a liquid scintillation counter with an external standard correction (Packard Instruments). The counter was programmed to measure radioactivity as long as needed to reach a coefficient of variation (CV) of ≤1% in each sample. Known volumes of the labeled dextrose solution were treated

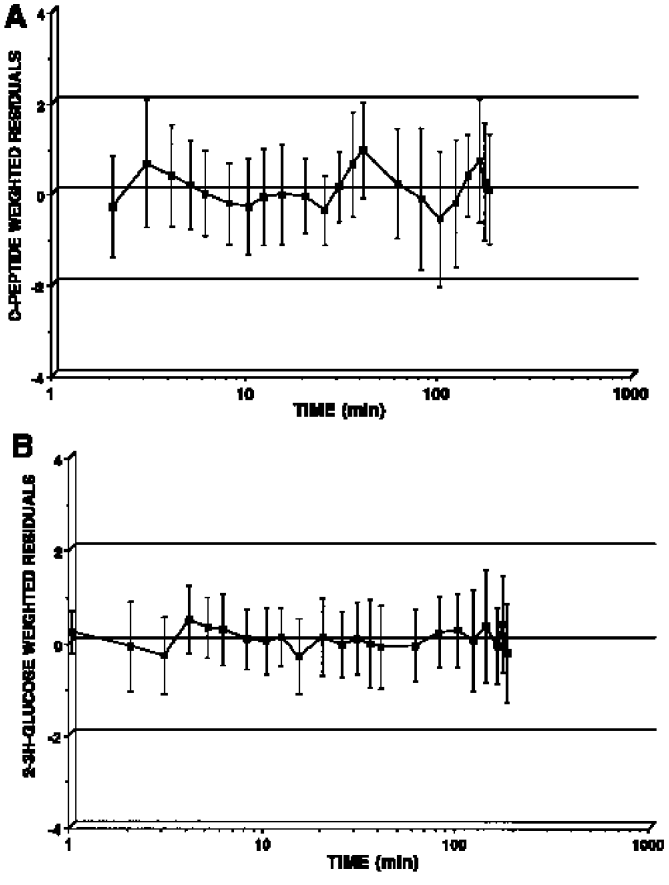

FIG. 1. Means ± SD of the weighted residuals of C-peptide (*A*) and [2-^{3}H]glucose (*B*) during the IVGTTs.

as previously described to determine the specific activity of the glucose infusates. Lactate and FFA plasma concentrations were determined with enzymic spectrophotometric methods, as previously described (43,44).

Plasma GlcN concentrations were measured by an HPLC method, as previously described (30).

Calculations. β-Cell secretion was estimated by applying a minimal model of glucose-induced insulin secretion to the glucose and C-peptide curves of each subject, as introduced by Toffolo et al. (45) and described in the APPENDIX (we have applied in the present article a simplified version of model 3 described in Appendix B of the article by Toffolo et al.). Readily releasable insulin (RRI) (pmol), glucose-stimulated insulin secretion (GSIS) ([pmol/min]/[mol/l]), glucose threshold (mmol/l), and the time constant (min) of GSIS were estimated by implementing this minimal model of C-peptide secretion in the SAAM II 1.1.1 software (SAAM Institute, Seattle, WA) (details are provided in the APPENDIX). Numerical values of the unknown parameters were estimated using nonlinear least-squares. Weights were chosen optimally: they were equal to the inverse of the variance of the measurement errors, which were assumed to be additive, uncorrelated with 0 mean and a constant CV of 6%. In all cases, the fit was good, as shown by the C-peptide weighted residuals (Fig. 1), and the parameters of glucose-induced β-cell secretion were estimated with good precision, as shown by their CVs (RRI 12.3 ± 3.3, GSIS 14.5 ± 4.3, and the glucose threshold 2.1 ± 0.7%).

The insulin and [2-^{3}H]glucose curves during the IVGTT were analyzed according to the minimal model described by Vicini et al. (46), with the aid of the SAAM II 1.1.1 software (details are provided in the APPENDIX). Numerical values of the unknown parameters were estimated using nonlinear least-squares. Weights were chosen optimally: they were equal to the inverse of the variance of the measurement errors, which were assumed to be additive, uncorrelated with 0 mean and a constant CV of 3%. The relevant parameters obtained with this analysis were insulin sensitivity (S_I) under hyperglycemic/hyperinsulinemic conditions (S_I*-IVGTT [ml · min^{-1} · kg^{-1}]/[pmol/l]), glucose effectiveness (S_G*) (ml · min^{-1} · kg^{-1}) at basal steady-state insulinemia, and the plasma glucose clearance rate at baseline (ml · min^{-1} · kg^{-1}), which was used to calculate the rate of basal endogenous glucose output (EGO). The fit of the [2-^{3}H]glucose curve was good in all of the

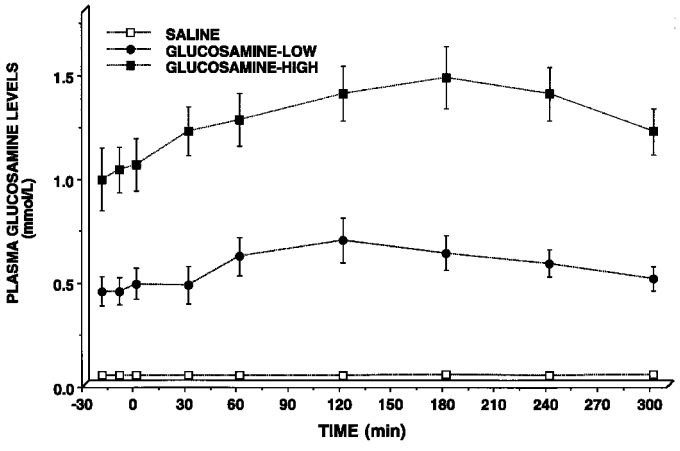

FIG. 2. Plasma GlcN levels during the saline, the low GlcN, and the high GlcN studies.

studies, as shown by the [2-^{3}H]glucose weighted residuals (Fig. 1). The CVs of S_I*-IVGTT (14.4 ± 3.4%), S_G* (15.1 ± 4.2%), and the plasma glucose clearance rate (6.14 ± 1.5%) were also good.

We also estimated EGO (μmol · min^{-1} · kg^{-1}) at baseline and over 10-min intervals during the IVGTT, as described in the APPENDIX.

Glucose utilization (μmol · min^{-1} · kg^{-1}) and EGO during the insulin clamp were measured in the time interval between 240 and 300 min, when isotopic near–steady state was present, according to standard formulae (43).

Glucose and lipid oxidation rates (μmol · min^{-1} · kg^{-1}) were estimated from gaseous exchange data by applying standard stoichiometric formulas, the theoretical underpinnings and limitations of which have been examined elsewhere (43,47). Glucose storage, also known as nonoxidative glucose disposal (43), was calculated as follows:

Glucose storage (μmol · min^{-1} · kg^{-1}) =
glucose utilization – glucose oxidation

Statistical analysis. The weighted residuals of serum C-peptide and plasma [2-^{3}H]glucose data are presented as means ± SD (Fig. 1). All other data are presented as means ± SE. The time courses of glucose, C-peptide, insulin, and [2-^{3}H]glucose concentrations; of EGO during the IVGTT; of plasma lactate and FFA levels during the insulin clamp; and of plasma GlcN concentrations throughout the study were compared by 1-way analysis of variance (ANOVA) for repeated measures. RRI, GSIS, the glucose threshold, the time constant of GSIS, S_I*-IVGTT, S_G*, and metabolic fluxes were compared using Student's t test for paired data.

The minimal detectable difference of a variable of interest in a paired study was calculated according to the following:

$$\delta = s \times (t_{a(2)m} + t_{b(1)m})/(n^{1/2})$$

where δ is the minimal detectable fractional difference, s is the fractional CV of the variable, $t_{b(1)m}$ and $t_{a(2)m}$ are the t values corresponding to a 90% (1 – β) chance of detecting a 0.05 [α(2)] level of significance with m degrees of freedom, and n is the number of observations (48).

RESULTS

GlcN, glucose, insulin, and C-peptide concentrations. During the saline study, the mean plasma GlcN concentration was 0.040 ± 0.007 mmol/l. During the low GlcN and the high GlcN studies, plasma GlcN concentrations increased to 0.57 ± 0.14 mmol/l (P < 0.01 vs. the saline study) and 1.15 ± 0.18 mmol/l (P < 0.001 vs. the saline study, and P < 0.01 vs. the low GlcN study, respectively) (Fig. 2). GlcN excretion rates in the urine samples were 0.055 ± 0.01 (n = 3), 0.46 ± 0.16 (n = 3), and 1.99 ± 0.28 μmol · min^{-1} · kg^{-1} (n = 4) in the saline, low GlcN, and high GlcN studies, respectively.

The mean plasma glucose concentration at baseline (–20 to 0 min) was 5.0 ± 0.04 mmol/l in the saline study and

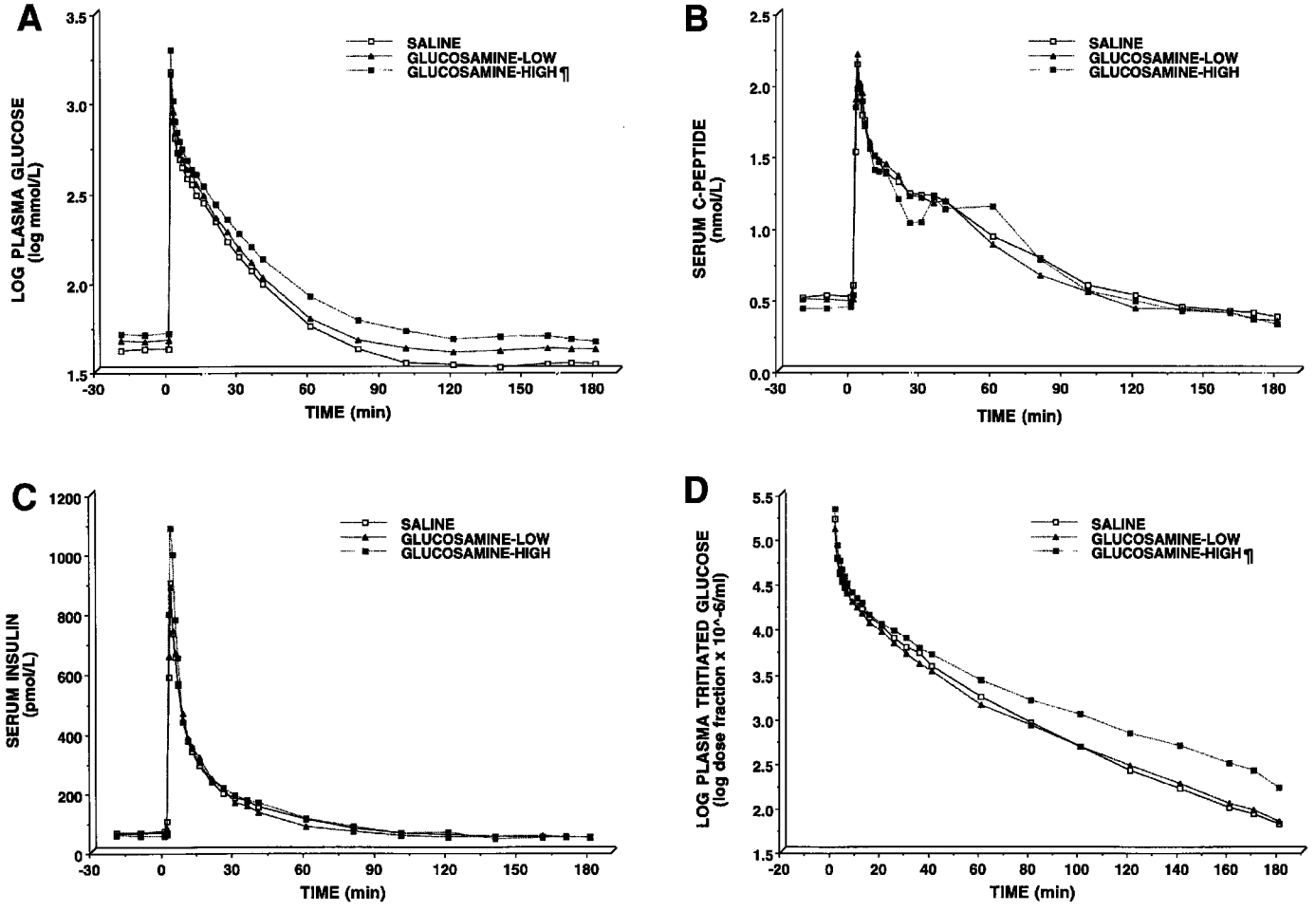

FIG. 3. Mean plasma glucose (*A*), serum C-peptide (*B*), serum insulin (*C*), and plasma [2-^{3}H]glucose (*D*) levels during the IVGTTs of the saline, the low GlcN, and the high GlcN studies. For the sake of clarity, SE bars have been omitted. ¶*P* < 0.01 for the high GlcN vs. the saline study by (determined by ANOVA).

increased to 5.3 ± 0.02 mmol/l (***P*** < 0.02) and 5.5 ± 0.01 mmol/l (***P*** < 0.05) in the low GlcN and the high GlcN studies, respectively. Insulin and C-peptide concentrations at baseline (–20 to 0 min) were 59 ± 5.2 pmol/l and 0.51 ± 0.02 nmol/l, respectively, in the saline study, and they were unchanged during both the low GlcN study (55 ± 3.5 pmol/l and 0.52 ± 0.05 nmol/l, respectively) and the high GlcN study (47.9 ± 1.6 pmol/l and 0.43 ± 0.01 nmol/l, respectively).

The plasma glucose concentration curve during the IVGTT in the high, but not in the low, GlcN study was somewhat greater than that in the saline study (***P*** < 0.01 by ANOVA), which indicated a worsening in glucose tolerance (Fig. 3). GlcN infusion caused no statistically significant differences in serum insulin and C-peptide curves during the IVGTTs (Fig. 3). However, the plasma [2-^{3}H]glucose curve during the IVGTT in the high, but not in the low, GlcN study was higher than that in the saline study (Fig. 3) (***P*** < 0.01 by ANOVA), suggesting a reduced clearance of the glucose load.

Parameters of β-cell secretion during the IVGTT. RRI was unaffected by GlcN infusion either at the low (***n*** = 10) or high (***n*** = 5) dose (Fig. 4). Similarly, GSIS, though somewhat reduced, was not statistically different during GlcN infusion compared with that in the saline study (Fig. 4). The time constant of GSIS (11.8 ± 2.3 min) was unaffected by either low (9.5 ± 1.7) or high (12.4 ± 4.2) GlcN infusion. In contrast, the glucose threshold for GSIS was significantly increased by GlcN administration in both studies (Fig. 4).

S_I, S_G*, and EGO during the IVGTT. S_I and S_G* during the saline study were 0.0210 ± 0.0056 [ml · min^{-1} · kg^{-1}]/[pmol/l] and 0.631 ± 0.12 ml · min^{-1} · kg^{-1}, respectively, and were unaffected by the low GlcN infusion (0.0174 ± 0.0037 [ml · min^{-1} · kg^{-1}]/[pmol/l] and 0.824 ± 0.16 ml · min^{-1} · kg^{-1}, respectively). However, high doses of GlcN (***n*** = 5) significantly blunted both S_I (0.0147 ± 0.0066 [ml · min^{-1} · kg^{-1}]/[pmol/l], ***P*** < 0.02) and S_G* (0.375 ± 0.15 ml · min^{-1} · kg^{-1}, ***P*** < 0.05) (Fig. 5).

EGO was unaffected by either low or high GlcN infusion, both at baseline and during the IVGTT (Fig. 6).

S_I and EGO during the insulin clamp. During the glucose clamp study, similar levels of plasma glucose and serum insulin were achieved during the saline study (4.91 ± 0.3 mmol/l and 501 ± 12.1 pmol/l), the low GlcN study (4.96 ± 0.2 mmol/l and 489 ± 11.6 pmol/l), and the high GlcN study (4.97 ± 0.2 mmol/l and 554 ± 39.5 pmol/l).

Both whole-body glucose utilization (Fig. 7) and EGO (2.26 ± 0.87, 2.72 ± 0.58, and 1.95 ± 0.65 μmol · min^{-1} · kg^{-1} for the saline, low GlcN, and high GlcN studies, respectively, NS) during systemic hyperinsulinemia were unaffected by GlcN infusion, regardless of the dose. Similarly, rates of glu-

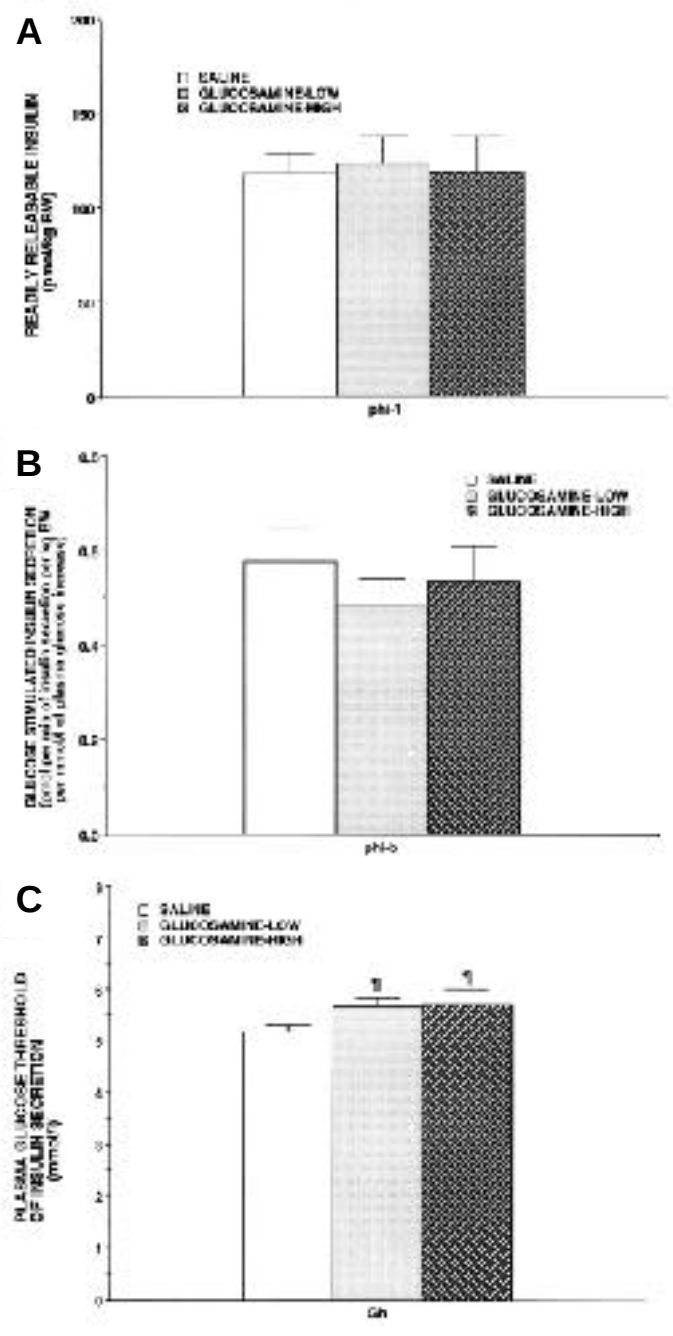

FIG. 4. RRI (*A*), GSIS (*B*), and the glucose threshold of GSIS (*C*) in the IVGTTs performed during the saline, the low GlcN, and the high GlcN studies. ¶*P* < 0.05 vs. the saline study.

cose oxidation and glucose storage stayed the same during GlcN administration (Fig. 7).

GlcN infusion at either dose exerted no effects on the time courses of both lactate and FFA concentrations (data not shown). Lipid oxidation rates were unchanged by GlcN infusion (data not shown).

DISCUSSION

The current status of the glucose toxicity hypothesis implies an involvement of the GlcN-hexosamine pathway in the detrimental effects of high glucose on both insulin secretion and insulin action, as previously described.

In the present study, GlcN was administered to humans (Fig. 2) in an attempt to prove that it can blunt the β-cell response to glucose in vivo. At variance with previous studies conducted in the rat (17,37,38), no alterations of the β-cell secretory pattern were observed during either the low- or the high-GlcN studies. However, GlcN shifted the β-cell glucose threshold to the right (Fig. 4). The expected net result of this alteration would be an increase in fasting glycemia, as observed during the studies performed with GlcN.

According to current thought, GlcN would impair GSIS by acting as a competitive inhibitor of β-cell glucokinase (17,37,38), which is the β-cell "glucose sensor" and the main regulatory step of GSIS (49). If GlcN acts as a pure competitive inhibitor of glucokinase, its predicted effect would be an increase in the apparent $\boldsymbol{K}_m$ of the enzyme for glucose and a shift to the right of the curve relating glucokinase flux to glucose concentration, but with no change in the shape of the curve. In our experimental setting, such a defect would manifest itself as an increase in the glucose threshold (i.e., a shift to the right of the relationship between glucose and insulin secretion), but no change would occur in the slope of this relationship (i.e., in GSIS). Thus, our data (Fig. 4) are consistent with the pattern expected with a competitive inhibitor of glucokinase. For the sake of comparison, subjects with the relatively mild glucokinase mutation E300Q display only a defect in the $\boldsymbol{K}_m$ of the enzyme with preserved V_{max}. Their in vivo GSIS is characterized by a shift to the right (i.e., an increase in glucose threshold) but a normal slope relating glucose levels to insulin secretion, at least in the glucose range between 7 and 12 mmol/l (50). As a result, their in vivo GSIS, at least qualitatively, is reminiscent of the defect in β-cell function induced by GlcN in the present study.

Previous studies in the rat have documented a clearer detrimental effect of GlcN on insulin secretion than that which is shown in humans in the present study (17,37,38), perhaps pointing to species-specific differences in the effects exerted by GlcN on insulin secretion. Indeed, in the rat, GlcN also impairs first-phase insulin secretion (17,37,38), a finding that is not expected with a competitive inhibitor of glucokinase. In comparison with our study, RRI was unaffected by GlcN (Fig. 4). These aspects need to be further investigated.

Our study is the first attempt in vivo in humans to increase the hexosamine pathway flux by infusing GlcN. Whereas no detectable effect could be documented on peripheral $\boldsymbol{S}_I$ at the low GlcN dose, at the high GlcN dose, $\boldsymbol{S}_I$ was decreased during hyperglycemia (IVGTT) (Fig. 5) but not at euglycemia (insulin clamp) (Fig. 7). Furthermore, $\boldsymbol{S}_G$* was also impaired during the IVGTT (Fig. 5). Thus, the ambient glucose levels determined whether GlcN could impair glucose utilization.

Glucose utilization during an IVGTT is governed by 2 components: one is ascribed to $\boldsymbol{S}_I$, and the other is ascribed to $\boldsymbol{S}_G$* (46). However, because the latter is estimated at basal insulin (46), additional effects of glucose on its own metabolism during hyperglycemia/hyperinsulinemia are reflected by $\boldsymbol{S}_I$. During clamp studies, glucose exerts a greater-than-expected potentiating effect on peripheral (muscle) uptake at increasing levels of hyperinsulinemia (51). The mechanism may be an increase in cell-surface GLUT activity induced by glucose, possibly through a protein kinase $C\beta_2$–dependent pathway (52) or through a stimulation of GLUT4 translocation in skeletal muscle (53). Also, liver may play a role, because even though the rate of liver glucose phosphoryla-

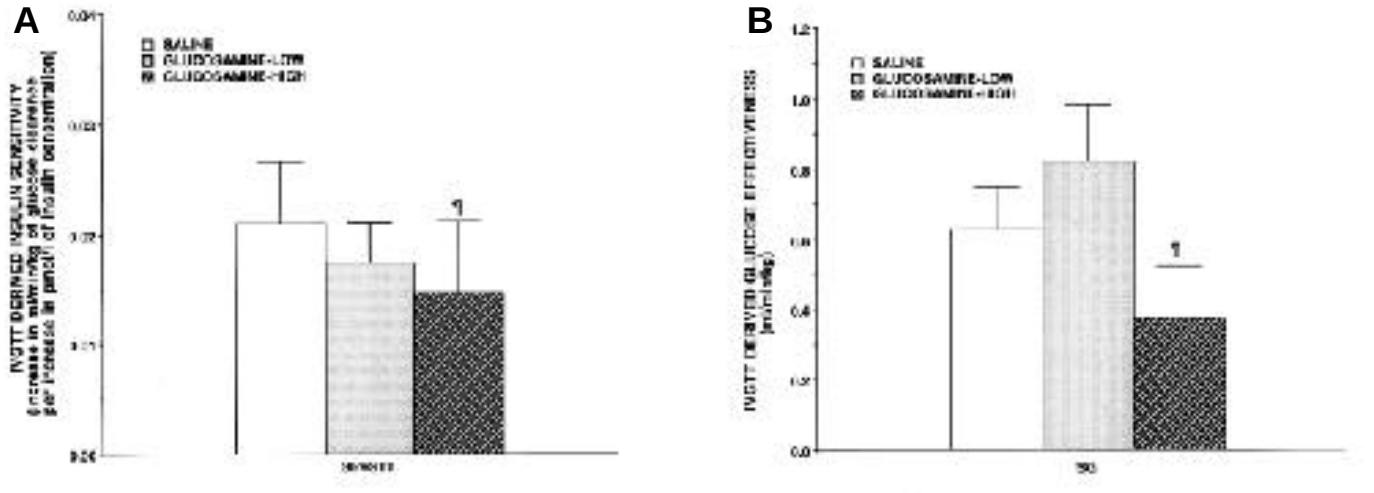

FIG. 5. S_I (*A*) and S_G* at basal insulin (*B*) derived from minimal model analysis of the IVGTTs performed during the saline, the low GlcN, and the high GlcN studies. ¶*P* < 0.05 vs. the saline study.

tion is almost negligible during a euglycemic clamp (54), liver glucose uptake accounts for ~30% of total glucose uptake during moderate hyperglycemia/hyperinsulinemia (55). Importantly, GlcN can inhibit liver glucokinase (35,56,57), thereby leading to a reduced rate of glucose phosphorylation in liver and a reduction in glucose cycling (56). Recently, a defect in S_G*, in which muscle and/or liver may be involved, was shown in type 2 diabetic patients during hyperinsulinemia only for glucose levels equaling 160 mg/dl (58). Thus, the defect in S_I during the IVGTT that is caused by GlcN is likely to be the result of an alteration in either peripheral or glucokinase-dependent liver glucose uptake (or both), which becomes evident only during hyperglycemia and is reminiscent of a specific defect in glucose metabolism, as recently described in type 2 diabetes (58).

The GlcN-induced decrease in S_G* at basal insulin (Fig. 5) is similar to the blunted effect of glucose on its own metabolism, as we (59) and other investigators (60,61) have previously reported in studies of type 2 diabetes. The possible determinants of this phenomenon may be a decreased basal clearance of glucose across the splanchnic area (62) and skeletal muscle (63). Our data therefore show that in humans, GlcN sets in motion a series of events (i.e., impaired β-cell function and reduced capability to clear a glucose load) that may be detrimental to glucose homeostasis.

The lack of any GlcN effect on glucose metabolism during the euglycemic clamp in humans (Fig. 7) is at variance with all of the published experimental evidence obtained in rodents (7,13,14,16–21,25,32,34).

A possible reason for this variance is that our study lacked statistical power to detect biologically significant alterations in S_I. In our laboratory, a 2-h euglycemic clamp in humans has a between-day CV of ~12%. Thus, according to the formula reported in the statistical analysis, we had an 80% chance of detecting a 10% difference at a level of $P < 0.05$. We may have missed smaller changes in S_I at euglycemia, but the biological significance of these changes would be questionable.

Another relevant issue concerns the doses of GlcN that we used. The low dose (1.6 μmol · min^{-1} · kg^{-1} body wt) was selected on the basis of the present estimates of the flux through the hexosamine pathway (~2–3% of basal glucose utilization [i.e., 0.2–0.4 μmol · min^{-1} · kg^{-1}]). Because ~30% of the

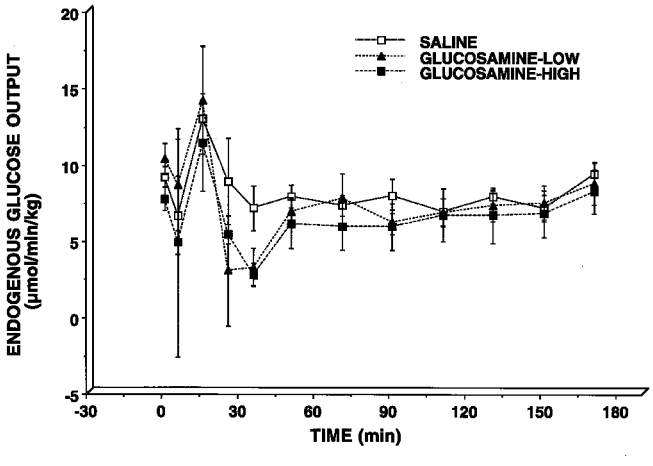

FIG. 6. Time course of EGO during the IVGTTs of the saline, the low GlcN, and the high GlcN studies.

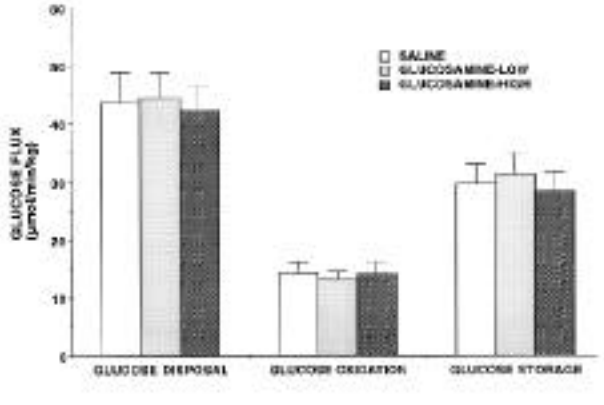

FIG. 7. Whole-body glucose disposal, glucose oxidation, and glucose storage in the last hour of the euglycemic-hyperinsulinemic clamps performed during the saline, the low GlcN, and the high GlcN studies.

GlcN infused was found in the urine, we may have accelerated the hexosamine pathway flux from a minimum of 2.7- to a maximum of 5.5-fold in the low GlcN study. The high GlcN dose (5 µmol · min^{-1} · kg^{-1}) has proven to be effective in inducing peripheral insulin resistance in the rat, both in our (17) and other investigators' (7,21,25) laboratories. It should have increased the hexosamine pathway flux from a minimum of 7.5- to a maximum of 15-fold. If one takes into account the ratio between GlcN dose and insulin-mediated uptake in rats and humans, our high GlcN study (ratio of ~1:8 between GlcN infusion and glucose uptake) used a dose that is comparable with the highest GlcN dose applied to the rat (30µmol · min^{-1} · kg^{-1}, ratio of ~1:7). Finally, the GlcN levels we achieved in the high GlcN study (~1.15 mmol/l) were even greater than those observed at the highest dose used in the rat (~0.8 mmol/l) (14). Nevertheless, all of the considerations regarding the flux rate through the hexosamine pathway are based on rat studies, not human studies, and we did not measure any metabolite of the hexosamine-phosphate pathway in the muscle of our subjects, thereby providing no definitive proof that the pathway flux was accelerated by GlcN infusion. Thus, although we deem it unlikely that the failure of GlcN to cause insulin resistance during our insulin clamp studies is due to an inadequate GlcN load, this possibility cannot be ruled out.

Another possible factor to examine is the time of exposure of body tissue to GlcN. In the rat, we and other investigators (7,17,25) reported that the detrimental effects of GlcN on insulin sensitivity were readily detectable with little lag time, whereas in other studies (16,18–20), GlcN was an effective insulin desensitizer after only 3–4 h of infusion. In our study, however, the body was exposed to hyperglucosaminemia for 5 h (Fig. 2) before we measured insulin sensitivity by the insulin clamp; yet no changes could be detected. In spite of this result, our data cannot be regarded as proof that the hexosamine pathway is not a flux sensor (4,24,25) and/or that GlcN does not cause insulin resistance at euglycemia in humans. Rather, our data show that the quantitative role, the sensitivity, or the timing of activation of the GlcN/hexosamine pathway in modulating peripheral insulin sensitivity at euglycemia is different in rats and in humans. Consequently, these findings call for some caution in the prompt extrapolation of rodent data to human homeostatic mechanisms.

In cultured cells and also in vivo in the rat, GlcN can selectively inhibit glycogen synthesis by virtue of a direct effect on the degree of phosphorylation of glycogen synthase (9–11). We observed no changes in the rates of glucose storage during GlcN studies (Fig. 7), a parameter that is closely related to glycogen synthesis at both the whole-body (43) and the muscular level (64). A decrease in glycogen synthesis may have been offset by an increase in anaerobic glycolysis, which is similarly encompassed in the rate of glucose storage (43). In such a case, we should have observed an increase in lactate levels, but we did not. Thus, we think that this selective effect on intracellular glucose partitioning did not occur in our studies.

GlcN may decrease glucose capability of restraining endogenous glucose production by virtue of an inhibition on liver glucokinase, as demonstrated in the rat (56). However, to avoid tracer recirculation, we were forced to use [2-^{3}H]glucose, which quantitates total EGO (i.e., total glucose-6-phosphatase flux), not glucose production (i.e., the net balance between glucose-6-phophatase and glucokinase fluxes). Under our experimental conditions, GlcN does not affect EGO in humans. However, we used an insulin dose that shuts off EGO almost completely. The issue of whether GlcN can affect liver (kidney) glucokinase and endogenous glucose production needs to be investigated.

In summary, we observed that GlcN administered acutely in vivo in humans can induce a mild dysfunction in β-cell secretion (Fig. 4), and, at a higher dose, an impairment in glucose utilization under hyperglycemic/hyperinsulinemic conditions and a decrease in $\boldsymbol{S}_G$* at basal insulinemia (Fig. 5). The first 2 effects are consistent with the notion that GlcN can act as a competitive inhibitor of glucokinase in the β-cell (36,37) and in glucose-producing organs (35,56), although a defect in peripheral glucose uptake is also likely to be involved (51–53). The net result of these alterations was a small increase in fasting glucose levels and a worsening of glucose tolerance (Fig. 3) (i.e., a mild but detectable disruption of glucose homeostasis). This scenario recapitulates some of the metabolic features of human diabetes (65) and lends support to the thesis that inappropriate hexosamine metabolism can adversely affect glucose homeostasis (4,17,24,25).

However, in contrast to the rodent studies (7,13,14,16–21, 25,32,34), GlcN caused no detectable effects on insulin-mediated glucose metabolism at euglycemia (Fig. 7), suggesting that caution is still warranted in extrapolating the animal data to the human setting in this specific topic. Further studies will be needed to determine whether acute acceleration of the hexosamine biosynthetic pathway can induce in vivo insulin resistance in humans under the standard conditions of the insulin clamp.

ACKNOWLEDGMENTS

This work was supported by grants to R.C.B. from the Consiglio Nazionale delle Ricerche and the Società Italiana di Diabetologia.

Monica Zardini and Federica Moschetta provided superb technical help.

APPENDIX

Minimal model of C-peptide secretion. The analysis of the glucose and C-peptide curves (Fig. 3) during the IVGTT follows the general strategy proposed by Toffolo et al. (45) (Fig. A1). Briefly, C-peptide kinetics are assumed to be known in each subject, according to a 2-compartment model proposed by Polonsky et al. (66). Individual parameters can be calculated from population data as indicated by Van Cauter et al. (67). C-peptide secretion is appended to this model of C-peptide kinetics and is assumed to consist of 2 components. The first phase (pmol/kg) is described as a pulse bolus of C-peptide at 0 min in response to the sudden hyperglycemic stimulus. The second phase also starts at 0 min and is described by the following:

$$SR(\boldsymbol{t}) = \tau^{-1} \times \boldsymbol{X}(\boldsymbol{t})$$

$$\frac{d\boldsymbol{X}(\boldsymbol{t})}{d\boldsymbol{t}} = -\tau^{-1} \times \boldsymbol{X}(\boldsymbol{t}) + \beta[\boldsymbol{G}(\boldsymbol{t}) - \boldsymbol{h}]$$

$$\boldsymbol{X}(0) = 0$$

where SR($\boldsymbol{t}$) is the secretion rate (pmol · min^{-1} · kg^{-1}) of C-peptide, τ (min) is the time constant with which the amount of C-peptide made available for secretion is released

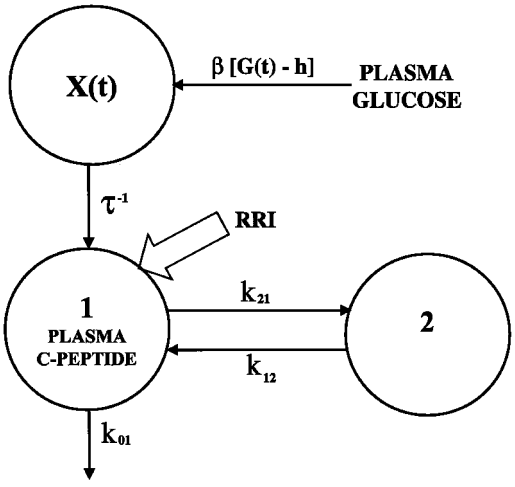

FIG. A1. Structure of the minimal model of insulin (C-peptide) secretion used in the present article to quantify β-cell responses to glucose during the IVGTT.

into the circulation, $X(t)$ is the amount of C-peptide made available for secretion by the glucose stimulus, β ([pmol · min^{-1} · kg^{-1}]/[mmol/l]) is the slope of the straight line that relates plasma glucose (mmol/l) to the provision of C-peptide (pmol · min^{-1} · kg^{-1}) to the secretory process, $G(t)$ is the prevailing plasma glucose level (mmol/l), and h is the plasma glucose threshold (mmol/l), above which the second phase of insulin secretion starts.

The parameters defining β-cell sensitivity to glucose are defined as follows: ***1***) first-phase secretion, referred to in the present article as RRI (pmol/kg); ***2***) β, also named Φ2 (45), which is referred to in the present article as GSIS ([pmol · min^{-1} · kg^{-1}]/[mmol/l]); ***3***) the time constant (min) of second-phase secretion; and ***4***) the glucose threshold of GSIS (mmol/l).

Minimal model of glucose metabolism. We have applied the same modeling strategy described by Vicini et al. (46). The decay curve of [2-^{3}H]glucose after a labeled IVGTT and the plasma insulin curve (Fig. 3) are used to identify the kinetics of [2-^{3}H]glucose utilization and the control exerted by insulin on this utilization.

The glucose system is formed by 2 compartments in bidirectional exchange with each other (Fig. A2). Compartment 1 is the fast glucose compartment, where the injection and the sampling take place; compartment 2 is the slow glucose compartment. Glucose utilization in compartment 1 is entirely insulin-independent and is formed by 2 components. One is fixed (constant glucose uptake [CGU]) and concentration-independent within the range of euglycemia/hyperglycemia; it represents glucose utilization by brain and red blood cells, and it is assumed to be 204 μmol · min^{-1} · m^{-2} of body surface area. The other is proportional to glucose mass in compartment 1; it is described by the time-invariant rate constant k_{GD}. The rate constant (k_{01}) of the irreversible loss from the insulin-independent compartment, therefore, is time varying and equals:

$$k_{01} = k_{GD} + \frac{CGU}{q1}$$

where $q1$ is the glucose mass (μmol) in the insulin-independent compartment. Thus, if plasma glucose concentration varies, the rate constant k_{01} is also time-varying in the term CGU/$q1$.

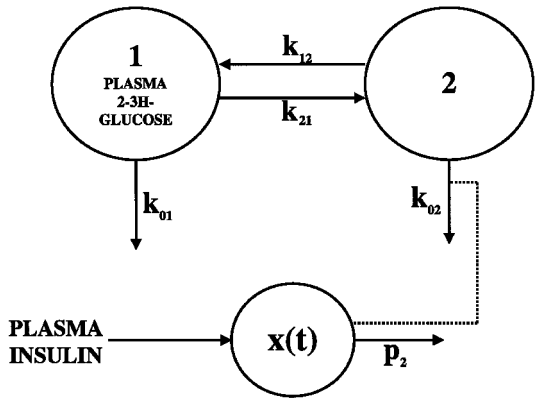

FIG. A2. Structure of the minimal model of glucose metabolism used in the present article to quantify S_I and S_G* during the IVGTT.

Glucose utilization in compartment 2 is formed by 2 components. One is insulin-independent and is proportional to glucose mass in compartment 2; it is described by the time-invariant rate constant k_{ID}. The other is the time-varying insulin-dependent glucose utilization. It is assumed that insulin action takes place in a compartment that is remote from plasma. Insulin action on glucose metabolism is described by the function $x(t)$:

$$\frac{dx(t)}{dt} = -p_2\,(x[t] - s_k \times [\,I(t) - I_b])$$

$$x(0) = 0$$

where p_2 is the parameter determining the fading of insulin action in the insulin remote compartment, s_k (ml · min^{-1} · pmol^{-1}) is the increase in glucose clearance from compartment 2 determined by a 1 pmol/l increase in plasma insulin concentration, $I(t)$ is the time course of plasma insulin concentration, and I_b is basal insulinemia.

The rate constant (k_{02}) of the irreversible loss from the insulin-dependent compartment, therefore, is time varying and equals:

$$k_{02} = k_{ID} + x(t)$$

Thus, if insulin concentration varies, the rate constant k_{02} is time varying also in the term $x(t)$.

By measuring the time courses of insulin and [2-^{3}H]glucose concentrations during an IVGTT in sufficient detail, this system is uniquely identifiable (46). The relevant parameters for glucose metabolism are S_I*-IVGTT ([ml/min]/[pmol/l]) and S_G* (ml/min) at basal steady-state insulinemia. The equations for both are respectively:

$$S_G^* = V_1\,[k_p + (k_{21}k_{02})/(k_{02} + k_{12})]$$

$$S_I = V_1 s_k\,[(k_{21}k_{12})/(k_{02} + k_{12})^2]$$

In this article, both of parameters, S_I and S_G*, were normalized per kilogram of body weight. Another important parameter that can be estimated with the aid of this model (46) is the plasma glucose clearance rate (ml/min) at baseline:

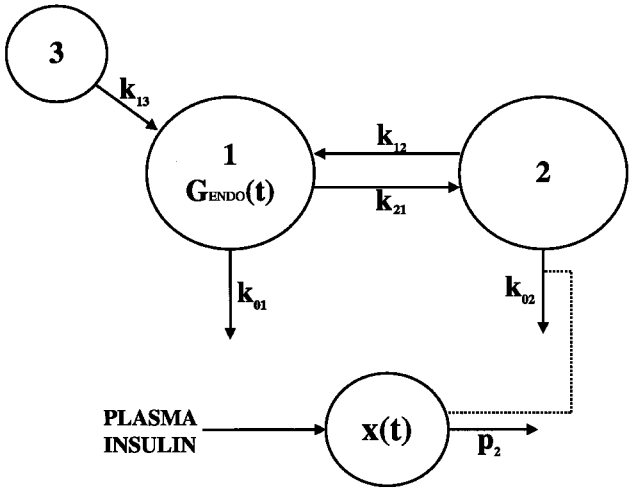

FIG. A3. Structure of the minimal model of glucose metabolism used to estimate EGO from endogenous glycemia data ($G_{ENDO}[t]$) in the present article.

Plasma glucose clearance rate =

$$V_1 \times [k_{01} + (k_{21}k_{02})/(k_{02} + k_{12})]$$

Multiplying the plasma glucose clearance rate by the basal plasma glucose concentrations provides an estimate of the basal glucose turnover rate (basal EGO and basal glucose utilization [$\mu mol \cdot min^{-1} \cdot kg^{-1}$]).

EGO during the IVGTT. After identifying the insulin-[2-^{3}H]glucose system in each study, this information was used to obtain an estimate of EGO during the IVGTT. The plasma glucose response after the IVGTT, $G(t)$, was separated in 2 components (68): the theoretical response to the exogenous glucose bolus, $G_{EXO}(t)$, and the theoretical response to the EGO, $G_{ENDO}(t)$:

$$G_{EXO}(t)\ (\mu mol/ml) = \frac{[2\text{-}^3H]\text{glucose concentration (dpm/ml)}}{\text{specific activity of the glucose bolus (dpm/}\mu mol)}$$

$$G_{ENDO}(t) = G(t) - G_{EXO}(t)$$

$G_{ENDO}(t)$, or endogenous glucose, was smoothed with the 5-point moving average to reduce the noise of the estimated $G_{ENDO}(t)$ dynamics (69). The endogenous glucose represents the time course of plasma glucose when the only glucose source is the EGO.

To estimate EGO from $G_{ENDO}(t)$, the insulin-glucose system (Fig. A3) was added with a third compartment, which directly feeds compartment 1. The content of compartment 3 was arbitrarily fixed to 14 mol, a quantity that was chosen to make the change in glucose content in compartment 3 negligible over the 180-min duration of the IVGTT. Thus, the rate of glucose exit from compartment 3 is the rate of EGO and is proportional to the rate constant k_{13}. Because all other model parameters are known from the previous analysis of the insulin/[2-^{3}H]-D-glucose curves, and because glucose mass is fixed in compartment 3, the only parameter that was estimated to fit $G_{ENDO}(t)$ was k_{13}. The parameter k_{13} was therefore estimated on a point-to-point basis with the SAAM 1.1.1 software, which calculated the EGO that would perfectly fit each smoothed endogenous glucose point. This approach is not devoid of significant limitations (68,69). Indeed, significant swings, as expected, were observed in the initial part of the IVGTT study, when the dynamic changes in the D-glucose curves were maximal (Figs. 3 and 6).

REFERENCES

1. Unger RH, Grundy S: Hyperglycemia as an inducer as well as a consequence of impaired islet function and insulin resistance: implications for the management of diabetes. ***Diabetologia*** 28:119–121, 1985
2. Rossetti L, Giaccari A, DeFronzo RA: Glucose toxicity. ***Diabetes Care*** 13:610–630, 1990
3. Traxinger RR, Marshall S: Role of amino acids in modulating glucose-induced desensitization of the glucose transport system. ***J Biol Chem*** 35:20910–20916, 1989
4. Marshall S, Bacote V, Traxinger RR: Discovery of a metabolic pathway mediating glucose-induced desensitization of the glucose transport system: role of hexosamine biosynthesis in the induction of insulin resistance. ***J Biol Chem*** 266:4706–4712, 1991
5. Traxinger RR, Marshall S: Coordinated regulation of glutamine:fructose-6-phosphate amidotransferase activity by insulin, glucose, and glutamine: role of hexosamine biosynthesis in enzyme regulation. ***J Biol Chem*** 266:10148–10154, 1991
6. Nerlich AG, Sauer U, Kolm Litty V, Wagner E, Koch M, Schleicher ED: Expression of glutamine:fructose-6-phosphate amidotransferase in human tissues: evidence for high variability and distinct regulation in diabetes. ***Diabetes*** 47:170–178, 1998
7. Baron AD, Zhu JS, Zhu JH, Weldon H, Maianu L, Garvey WT: Glucosamine induces insulin resistance in vivo by affecting GLUT 4 translocation in skeletal muscle: implications for glucose toxicity. ***J Clin Invest*** 96:2792–2801, 1995
8. Cooksey RC, Hebert LF Jr, Zhu JH, Wofford P, Garvey WT, McClain DA: Mechanism of hexosamine-induced insulin resistance in transgenic mice overexpressing glutamine:fructose-6-phosphate amidotransferase: decreased glucose transporter GLUT4 translocation and reversal by treatment with thiazolidinedione. ***Endocrinology*** 140:1151–1157, 1999
9. Robinson KA, Sens DA, Buse MG: Pre-exposure to glucosamine induces insulin resistance of glucose transport and glycogen synthesis in isolated rat skeletal muscle: study of mechanisms in muscle and in rat-1 fibroblast overexpressing the human insulin receptor. ***Diabetes*** 42:1333–1346, 1993
10. Crook ED, Zhou J, Daniels M, Neidigh JL, McClain DA: Regulation of glycogen synthase by glucose, glucosamine, and glutamine:fructose-6-phosphate amidotransferase. ***Diabetes*** 44:314–320, 1995
11. Crook ED, McClain DA: Regulation of glycogen synthase and protein phosphatase-1 by hexosamines. ***Diabetes*** 45:322–327, 1996
12. Hresko RC, Heimberg H, Chi MM, Mueckler M: Glucosamine-induced insulin resistance in 3T3-L1 adipocytes is caused by depletion of intracellular ATP. ***J Biol Chem*** 273:20658–20668, 1998
13. Kim YB, Zhu JS, Zierath JR, Shen HQ, Baron AD, Kahn BB: Glucosamine infusion in rats rapidly impairs insulin stimulation of phosphoinositide 3-kinase but does not alter activation of Akt/protein kinase B in skeletal muscle. ***Diabetes*** 48:310–320, 1999
14. Patti ME, Virkamaki A, Landaker EJ, Kahn CR, Yki-Jarvinen H: Activation of the hexosamine pathway by glucosamine in vivo induces insulin resistance of early postreceptor insulin-signaling events in skeletal muscle. ***Diabetes*** 48:1562–1571, 1999
15. Filippis A, Clark S, Proietto J: Increased flux through the hexosamine biosynthesis pathway inhibits glucose transport acutely by activation of protein kinase C. ***Biochem J*** 324:981–985, 1997
16. Rossetti L, Hawkins M, Chen W, Gindi J, Barzilai N: In vivo glucosamine infusion induces insulin resistance in normoglycemic but not in hyperglycemic conscious rats. ***J Clin Invest*** 96:132–140, 1995
17. Giaccari A, Morviducci L, Zorretta D, Sbraccia P, Leonetti F, Caiola S, Buongiorno A, Bonadonna RC, Tamburrano G: In vivo effects of glucosamine on insulin secretion and insulin sensitivity in the rat: possible relevance to the maladaptive responses to chronic hyperglycemia. ***Diabetologia*** 38:518–524, 1995
18. Virkamaki A, Daniels MC, Hamalainen S, Utriainen T, McClain D, Yki-Jarvinen H: Activation of the hexosamine pathway by glucosamine in vivo induces insulin resistance in multiple insulin sensitive tissues. ***Endocrinology*** 138:2501–2507, 1997
19. Hawkins M, Barzilai N, Chen W, Angelov I, Hu M, Cohen P, Rossetti L: Increased hexosamine availability similarly impairs the action of insulin and IGF-1 on glucose disposal. ***Diabetes*** 45:1734–1743, 1996

20. Holmang A, Nilsson C, Niklasson M, Larsson BM, Lonroth P: Induction of insulin resistance by glucosamine reduces blood flow but not interstitial levels of either glucose or insulin. ***Diabetes*** 48:106–111, 1999
21. Hawkins M, Barzilai N, Liu R, Hu M, Chen W, Rossetti L: Role of the glucosamine pathway in fat-induced insulin resistance. ***J Clin Invest*** 99:2173–2182, 1997
22. Buse MG, Robinson KA, Marshall BA, Mueckler M: Differential effects of GLUT1 or GLUT4 overexpression on hexosamine biosynthesis by muscles of transgenic mice. ***J Biol Chem*** 271:23197–23202, 1996
23. Hebert LF Jr, Daniels MC, Zhou J, Crook ED, Turner RL, Simmons ST, Neidigh JL, Zhu JS, Baron AD, McClain DA: Overexpression of glutamine:fructose-6-phosphate amidotransferase in transgenic mice leads to insulin resistance. ***J Clin Invest*** 98:930–936, 1996
24. McClain DA, Crook ED: Hexosamines and insulin resistance. ***Diabetes*** 45:1003–1009, 1996
25. Wang J, Liu R, Hawkins M, Barzilai N, Rossetti L: A nutrient-sensing pathway regulates leptin gene expression in muscle and fat. ***Nature*** 393:684–688, 1998
26. Shimabukuro M, Koyama K, Vhen G, Wang M-Y, Trieu F, Lee Y, Newgard CB, Unger RH: Direct antidiabetic effect of leptin through triglyceride depletion of tissues. ***Proc Natl Acad Sci U S A*** 94:4637–4641, 1997
27. Robinson KA, Weinstein ML, Lindenmayer GE, Buse MG: Effects of diabetes and hyperglycemia on the hexosamine synthesis pathway in rat muscle and liver. ***Diabetes*** 44:1438–1446, 1995
28. Buse MG, Robinson KA, Gettys TW, McMahon EG, Gulve EA: Increased activity of the hexosamine synthesis pathway in muscles of insulin-resistant ***ob***/***ob*** mice. ***Am J Physiol*** 272: E1080–E1088, 1997
29. Yki-Jarvinen H, Daniels MC, Virkamaki A, Makimattila S, DeFronzo RA, McClain D: Increased glutamine:fructose-6-phosphate amidotransferase activity in skeletal muscle of patients with NIDDM. ***Diabetes*** 45:302–307, 1996
30. Daniels MC, Ciaraldi TP, Nikoulina S, Henry RR, McClain DA: Glutamine:fructose-6-phosphate amidotransferase activity in cultured human skeletal muscle cells: relationship to glucose disposal rate in control and non-insulin-dependent diabetes mellitus subjects and regulation by glucose and insulin. ***J Clin Invest*** 97:1235–1241, 1996
31. Shepherd PR, Kahn BB: Glucose transporters and insulin action: implications for insulin resistance and diabetes mellitus. ***N Engl J Med*** 341:248–257, 1999
32. Miles PDG, Higo K, Romeo OR, Lee M-K, Rafaat K, Olefsky JO: Troglitazone prevents hyperglycemia-induced but not glucosamine-induced insulin resistance. ***Diabetes*** 47:395–400, 1998
33. Nelson BA, Robinson KA, Koning JS, Buse MG: Effects of exercise and feeding on the hexosamine biosynthetic pathway in rat skeletal muscle. ***Am J Physiol*** 272:E848–E855, 1997
34. Virkamaki A, Yki-Jarvinen H: Allosteric regulation of glycogen synthase and hexokinase by glucosamine-6-phosphate during glucosamine-induced insulin resistance in skeletal muscle and heart. ***Diabetes*** 48:1101–1107, 1999
35. Spiro RG: The effect of ***N***-acetylglucosamine and glucosamine on carbohydrate metabolism in rat liver slices. ***J Biol Chem*** 233:546–550, 1958
36. Malaisse WJ, Lea MA, Malaisse-Lagae F: The effect of mannoheptulose on the phosphorylation of glucose and the secretion of insulin by islets of Langerhans. ***Metabolism*** 17:126–132, 1968
37. Balkan B, Dunning BE: Glucosamine inhibits glucokinase in vitro and produces a glucose-specific impairment of in vivo insulin secretion in rats. ***Diabetes*** 43:1173–1179, 1994
38. Shankar RR, Zhu JS, Baron AD: Glucosamine infusion in rats mimics the beta-cell dysfunction of non-insulin-dependent diabetes mellitus. ***Metabolism*** 47:573–577, 1998
39. Adams ME: Hype about glucosamine. ***Lancet*** 354:353–354, 1999
40. National Diabetes Data Group: Classification and diagnosis of diabetes mellitus and other categories of glucose intolerance. ***Diabetes*** 28:1039–1057, 1979
41. DeFronzo RA, Tobin JD, Andres R: Glucose clamp technique: a method for quantifying insulin secretion and resistance. ***Am J Physiol*** 237:E214–E223, 1979
42. Perseghin G, Ghosh S, Gerow K, Shulman GI: Metabolic defects in lean nondiabetic offspring of NIDDM parents: a cross-sectional study. ***Diabetes*** 46:1001–1009, 1997
43. Bonadonna RC, Del Prato S, Bonora E, Gulli G, Solini A, DeFronzo RA: Effects of physiological hyperinsulinemia on the intracellular metabolic partition of plasma glucose. ***Am J Physiol*** 265:E943–E953, 1993

43a. Somogyi M: Determination of blood sugar. ***J Biol Chem*** 160:69–73, 1945

44. Bonadonna RC, Del Prato S, Saccomani MP, Bonora E, Gulli G, Ferrannini E, Bier D, Cobelli C, DeFronzo RA: Transmembrane glucose transport in skeletal muscle of patients with non-insulin-dependent diabetes. ***J Clin Invest*** 92:486–494, 1993
45. Toffolo G, De Grandi F, Cobelli C: Estimation of β-cell sensitivity from intravenous glucose tolerance test C-peptide data: knowledge of the kinetics avoids errors in modeling the secretion. ***Diabetes*** 44:845–854, 1995
46. Vicini P, Caumo A, Cobelli C: The hot IVGTT two-compartment minimal model: indexes of glucose effectiveness and insulin sensitivity. ***Am J Physiol*** 273:E1024–E1032, 1997
47. Frayn KN: Calculation of substrate oxidation rates in vivo from gaseous exchange. ***J Appl Physiol*** 55:628–634, 1983
48. Zar J: ***Biostatistical Analysis***. Englewood Cliffs, NJ, Prentice Hall, 1984
49. Matschinsky FM, Glaser B, Magnuson MA: Pancreatic β-cell glucokinase: closing the gap between theoretical concepts and experimental realities. ***Diabetes*** 47:307–315, 1998
50. Sturis J, Kurland IK, Byrne MM, Mosekilde E, Froguel P, Pilkis SJ, Bell GI, Polonsky KS: Compensation in pancreatic β-cell function in subjects with glucokinase mutations. ***Diabetes*** 43:718–723, 1994
51. Yki-Jarvinen H, Young AA, Lamkin C, Foley JE: Kinetics of glucose disposal in whole body and across the forearm in man. ***J Clin Invest*** 79:1713–1719, 1987
52. Kawano Y, Rincon J, Soler A, Ryder JW, Nolte LA, Zierath JR, Wallberg-Henriksson H: Changes in glucose transport and protein kinase Cβ2 in rat skeletal muscle induced by hyperglycaemia. ***Diabetologia*** 42:1071–1079, 1999
53. Galante P, Mosthaf L, Kellerer M, Berti L, Tippmer L, Bossenmaier B, Fujiwara T, Okuno A, Horikoshi H, Häring HU: Acute hyperglycemia provides an insulin-independent inducer for GLUT4 translocation in C_2C_{12} myotubes and rat skeletal muscle. ***Diabetes*** 44:646–651, 1995
54. DeFronzo RA, Jacot E, Jequier E, Maeder E, Wahren J, Felber JP: The effects of insulin on the disposal of intravenous glucose: results from indirect calorimetry and hepatic and femoral venous catheterization. ***Diabetes*** 30:1000–1007, 1981
55. Saccà L, Orofino G, Petrone A, Vigorito C: Differential roles of splanchnic and peripheral tissues in the pathogenesis of impaired glucose tolerance. ***J Clin Invest*** 73:1683–1687, 1984
56. Barzilai N, Hawkins M, Angelov I, Hu M, Rossetti L: Glucosamine-induced inhibition of liver glucokinase impairs the ability of hyperglycemia to suppress endogenous glucose production. ***Diabetes*** 45:1329–1335, 1996
57. Cadefau J, Bollen M, Stalmans W: Glucose-induced glycogenesis in the liver involves the glucose-6-phosphate-dependent dephosphorylation of glycogen synthase. ***Biochem J*** 322:745–750, 1997
58. Nielsen MF, Basu R, Wise S, Caumo A, Cobelli C, Rizza RA: Normal glucose-induced suppression of glucose production but impaired stimulation of glucose disposal in type 2 diabetes: evidence for a concentration-dependent defect in uptake. ***Diabetes*** 47:1735–1747, 1998
59. Del Prato S, Matsuda M, Simonson DC, Groop LC, Sheehan P, Leonetti F, Bonadonna RC, DeFronzo RA: Studies on the mass action effect of glucose in NIDDM and IDDM: evidence for glucose resistance. ***Diabetologia*** 40:687–697, 1997
60. Basu A, Caumo A, Bettini F, Gelisio A, Alzaid A, Cobelli C, Rizza RA: Impaired basal glucose effectiveness in NIDDM: contribution of defects in glucose disappearance and production, measured using an optimized minimal model independent protocol. ***Diabetes*** 46:421–432, 1997
61. Avogaro A, Vicini P, Valerio A, Caumo A, Cobelli C: The hot but not the cold minimal model allows precise assessment of insulin sensitivity in NIDDM. ***Am J Physiol*** 270:E532–E540, 1996
62. DeFronzo RA, Ferrannini E, Hendler R, Felig P, Wahren J: Regulation of splanchnic and peripheral glucose uptake by insulin and hyperglycemia in man. ***Diabetes*** 32:35–45, 1983
63. Baron AD, Brechtel G, Wallace P, Edelman SV: Rates and tissues sites of non-insulin- and insulin-mediated glucose uptake in humans. ***Am J Physiol*** 255: E769–E774, 1988
64. Shulman GI, Rothman DL, Jue T, Stein P, DeFronzo RA, Shulman RG: Quantitation of muscle glycogen synthesis in normal subjects and subjects with non-insulin-dependent diabetes by ^{13}C-nuclear magnetic resonance. ***N Engl J Med*** 322:223–228, 1990
65. DeFronzo RA, Bonadonna RC, Ferrannini E: Pathogenesis of NIDDM. In ***International Textbook of Diabetes Mellitus***. 2nd ed. Alberti KGMM, DeFronzo RA, Zimmet P, Keen H, Eds. London, John Wiley and Sons, 1997, p. 635–712
66. Polonsky KS, Licinio-Paixao J, Given BD, Pugh W, Rue P, Galloway J, Karrison T, Frank B: Use of biosynthetic human C-peptide in the measurement of insulin secretion rates in normal volunteers and type I diabetic patients. ***J Clin Invest*** 77:98–105, 1986
67. Van Cauter E, Mestrez F, Sturis J, Polonsky KS: Estimation of insulin secretion rates from C-peptide levels: comparison of individual and standard kinetic parameters for C-peptide clearance. ***Diabetes*** 41:368–377, 1992
68. Caumo A, Cobelli C: Hepatic glucose production during the labeled IVGTT: estimation by deconvolution with a new minimal model. ***Am J Physiol*** 264:E829–E841, 1993
69. Steil GM, Rebrin K, Mittelman SD, Bergman RN: Role of portal insulin delivery in the disappearance of intravenous glucose and assessment of insulin sensitivity. ***Diabetes*** 47:714–720, 1998